# Electromagnetically induced grating in a four-level tripod-type atomic system*

Dong Ya-Bin(董雅宾)† and Guo Yao-Hua(郭耀华)

*Department of Physics, Shanxi University, Taiyuan* 030006, *China*

(Received 18 November 2013; revised manuscript received 24 February 2014; published online 28 May 2014)

An electromagnetically induced grating in a four-level tripod-type atomic system is studied theoretically. By virtue of a weak standing-wave signal field, the phase modulation effectively diffracts a weak probe field into the first-order direction. By changing the weak signal field, the diffraction of the weak probe field can be modulated in real time, and a first-order diffraction efficiency of more than 32% can be obtained with proper parameters. Such a system has a potential application in an all-optical switch controlled by a weak optical signal.

**Keywords:** electromagnetically induced grating, phase modulation, first-order diffraction efficiency

**PACS:** 42.50.Gy, 42.65.An **DOI:** 10.1088/1674-1056/23/7/074204

## 1. Introduction

As we all know, a resonant probe field should be absorbed strongly by the medium. When another field is added, coherent population trapping (CPT) is realized, in which case the extraction of the entire population is prevented.[1–3] Under CPT, the optical properties of the atomic medium can be manipulated readily. The medium can be made transparent to the probe field and electromagnetically induced transparency (EIT) is formed.[4] The theory based on EIT has been applied to many fields such as lasing without population inversion,[5,6] enhancement of refractive index,[7,8] slow light,[9,10] light storage,[11,12] nonlinear light generation,[13,14] atomic mirrors,[15,16] electromagnetically induced grating (EIG),[17–21] and other effects.[22–27]

Applying a standing-wave coupling field, the transparent and opaque regions appear alternately, so an amplitude grating was proposed.[17] The refraction property of the probe field is also changed by the coupling field, and a phase modulation is therefore introduced here. As a result, a phase grating was proposed in a three-level system.[17] The atomic grating realized by this system has been applied to all-optical switching and routing.[18] The intensities of higher-order diffraction maxima can also be enhanced in a three-level ladder-type system.[19] By introducing a microwave field, the diffraction efficiency can be further improved.[20] In addition, some schemes to realize the EIG were proposed for different atomic systems.[21,28]

In this paper, an EIG in a four-level tripod-type system is studied theoretically, and first-order diffraction efficiency of more than 32% is obtained, which is very close to that of an ideal sinusoidal phase grating. The first-order diffraction efficiency of the weak probe field can be controlled readily, and a weak signal can be used to modulate and switch the weak probe field.

In this article, we review some recent developments in the field of EIG. Section 2 introduces the theoretical model and equations. Section 3 discusses the results of theoretical simulation. In Section 4, we conclude and provide a look at potential developments.

## 2. The model and equations

Figure 1(a) illustrates the atomic model. It consists of a tripod-type four-level atom interacting with three laser fields. Levels $|1\rangle$, $|2\rangle$, and $|3\rangle$ are the ground states. Level $|4\rangle$ is an excited state that decays at a rate of $\Gamma$. A weak probe beam with a Rabi frequency $\Omega_{\rm p} = \mu_{41}E_{\rm p}/2\hbar$ couples to the transition $|1\rangle \leftrightarrow |4\rangle$. The levels $|2\rangle$ and $|4\rangle$ are connected by a coupling field with a Rabi frequency of $\Omega_{\rm c} = \mu_{42}E_{\rm c}/2\hbar$, while a signal wave with Rabi frequency $\Omega_{\rm s} = \mu_{43}E_{\rm s}/2\hbar$ is applied to the transition $|3\rangle \leftrightarrow |4\rangle$. Here $\mu_{41}$, $\mu_{42}$, and $\mu_{43}$ are the electric dipole moments between the corresponding states. If the signal wave is composed of two overlapping fields that form a standing wave in the $x$ direction (see Fig. 1(b)), then the signal Rabi frequency can be written as $\Omega_{\rm s}(x) = \Omega_{\rm s}\sin(\pi x/\Lambda)$, where $\Lambda$ represents the space period of the standing wave.

Under the dipole approximation and the rotational wave approximation, the interaction Hamiltonian $H_{\rm I}$ can be written as

$$\begin{aligned} H_{\rm I} = & -\hbar[(\Delta_{\rm p}-\Delta_{\rm c})|2\rangle\langle 2| + (\Delta_{\rm p}-\Delta_{\rm s})|3\rangle\langle 3| + \Delta_{\rm p}|4\rangle\langle 4|] \\ & -\hbar[\Omega_{\rm p}|4\rangle\langle 1| + \Omega_{\rm c}|4\rangle\langle 2| \\ & +\Omega_{\rm s}\sin(\pi x/\Lambda)|4\rangle\langle 3| + {\rm h.c.}], \end{aligned} \tag{1}$$

where $\Delta_{\rm p} = \omega_{\rm p} - \omega_{41}$, $\Delta_{\rm c} = \omega_{\rm c} - \omega_{42}$, and $\Delta_{\rm s} = \omega_{\rm s} - \omega_{43}$ are

*Project supported by the National Natural Science Foundation of China (Grants Nos. 11004126 and 61275212), the Natural Science Foundation of Shanxi Province, China (Grant No. 2011021003-1), and the National Basic Research Program of China (Grant No. 2010CB923102).

†Corresponding author. E-mail: ybdong@sxu.edu.cn

© 2014 Chinese Physical Society and IOP Publishing Ltd 

the detunings of the probe, coupling, and signal (standing) waves, respectively. Here, $\omega_{\rm p}$, $\omega_{\rm c}$, and $\omega_{\rm s}$ are the frequencies of the optical fields, while $\omega_{41}$, $\omega_{42}$, and $\omega_{43}$ are the corresponding atomic transition frequencies. Then we can obtain the equations of the density-matrix elements as

$$
\begin{aligned}
\dot{\rho}_{11} &= \mathrm{i}\Omega_{\rm p}^{*}\rho_{41} - \mathrm{i}\Omega_{\rm p}\rho_{14} + \Gamma_{41}\rho_{44},\\
\dot{\rho}_{21} &= [-\gamma_{21} + \mathrm{i}(\Delta_{\rm p} - \Delta_{\rm c})]\rho_{21} + \mathrm{i}\Omega_{\rm c}^{*}\rho_{41} - \mathrm{i}\Omega_{\rm p}\rho_{24},\\
\dot{\rho}_{31} &= [-\gamma_{31} + \mathrm{i}(\Delta_{\rm p} - \Delta_{\rm s})]\rho_{31} + \mathrm{i}\Omega_{\rm s}^{*}\sin(\pi x/\Lambda)\rho_{41} - \mathrm{i}\Omega_{\rm p}\rho_{34},\\
\dot{\rho}_{41} &= (-\gamma_{41} + \mathrm{i}\Delta_{\rm p})\rho_{41} + \mathrm{i}\Omega_{\rm p}(\rho_{11} - \rho_{44}) + \mathrm{i}\Omega_{\rm c}\rho_{21}\\
&\quad + \mathrm{i}\Omega_{\rm s}\sin(\pi x/\Lambda)\rho_{31},\\
\dot{\rho}_{22} &= \mathrm{i}\Omega_{\rm c}^{*}\rho_{42} - \mathrm{i}\Omega_{\rm c}\rho_{24} + \Gamma_{42}\rho_{44},\\
\dot{\rho}_{32} &= [-\gamma_{32} + \mathrm{i}(\Delta_{\rm c} - \Delta_{\rm s})]\rho_{32} + \mathrm{i}\Omega_{\rm s}^{*}\sin(\pi x/\Lambda)\rho_{42} - \mathrm{i}\Omega_{\rm c}\rho_{34},\\
\dot{\rho}_{42} &= (-\gamma_{42} + \mathrm{i}\Delta_{\rm c})\rho_{42} + \mathrm{i}\Omega_{\rm p}\rho_{12} + \mathrm{i}\Omega_{\rm c}(\rho_{22} - \rho_{44})\\
&\quad + \mathrm{i}\Omega_{\rm s}\sin(\pi x/\Lambda)\rho_{32},\\
\dot{\rho}_{33} &= \mathrm{i}\Omega_{\rm s}^{*}\sin(\pi x/\Lambda)\rho_{43} - \mathrm{i}\Omega_{\rm s}\sin(\pi x/\Lambda)\rho_{34} + \Gamma_{43}\rho_{44},\\
\dot{\rho}_{43} &= (-\gamma_{43} + \mathrm{i}\Delta_{\rm s})\rho_{43} + \mathrm{i}\Omega_{\rm p}\rho_{13} + \mathrm{i}\Omega_{\rm c}\rho_{23}\\
&\quad + \mathrm{i}\Omega_{\rm s}\sin(\pi x/\Lambda)(\rho_{33} - \rho_{44}),\\
\dot{\rho}_{44} &= \mathrm{i}\Omega_{\rm p}\rho_{14} - \mathrm{i}\Omega_{\rm p}^{*}\rho_{41} + \mathrm{i}\Omega_{\rm c}\rho_{24} - \mathrm{i}\Omega_{\rm c}^{*}\rho_{42}\\
&\quad + \mathrm{i}\Omega_{\rm s}\sin(\pi x/\Lambda)\rho_{34} - \mathrm{i}\Omega_{\rm s}^{*}\sin(\pi x/\Lambda)\rho_{43}\\
&\quad - (\Gamma_{41} + \Gamma_{42} + \Gamma_{43})\rho_{44},\\
\rho_{ji} &= (\rho_{ij})^{*}, \quad (i \neq j),\\
\rho_{11} + \rho_{22} + \rho_{33} + \rho_{44} &= 1,
\end{aligned}
\tag{2}
$$

where $\Gamma_{ij}$ is the population decay rate from level $i$ to $j$, and $\gamma_{ij}$ is the dephasing rate.

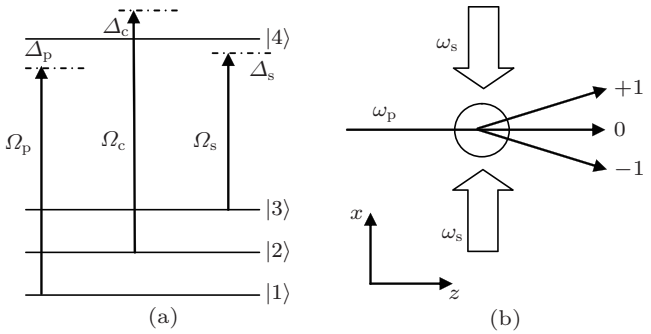



**Fig. 1.** (a) The atomic model. A tripod-type four-level atom interacting with three laser beams: probe ($\Omega_{\rm p}$), coupling ($\Omega_{\rm c}$), and signal ($\Omega_{\rm s}$). (b) Sketch of the probe- and signal-beam spatial configuration with respect to the atomic sample showing the zeroth and first diffraction orders.

Suppose the probe field is propagating along the $z$ direction through an extended atomic sample of length $L$. Under the slowly varying envelope approximation and the steady state regime, the propagation of the probe field is described by Maxwell's equation[17]

$$\frac{\partial E_{\rm p}}{\partial z} = \mathrm{i}\frac{k_{\rm p}}{2\varepsilon_0}P_{\rm p}, \tag{3}$$

where $P_{\rm p}$ is the slowly varying polarization. By performing a quantum average of the dipole moment over an ensemble of homogeneously broadened atoms, we can obtain $P_{\rm p} = 2N\mu_{41}\rho_{41}$, where $N$ is the atomic density. Substituting this expression for $P_{\rm p}$ into Eq. (3) yields

$$\frac{\partial \Omega_{\rm p}}{\partial z} = \mathrm{i}\frac{k_{\rm p}N\mu_{41}^{2}}{2\hbar\varepsilon_0}\rho_{41}. \tag{4}$$

In order to present the results in a unitless form, we choose $\gamma_{41}$ as the unit for all the Rabi frequencies, frequency detunings, and decay rates, and

$$z_0 = \frac{2\hbar\gamma_{41}\varepsilon_0}{Nk_{\rm p}\mu_{41}^{2}}, \tag{5}$$

which is the resonant absorption distance of the probe field in the absence of other fields as the unit for $z$.[17]

Then the equation for the probe field becomes

$$\frac{\partial \Omega_{\rm p}}{\partial z'} = (\alpha_{\rm r} + \mathrm{i}\alpha_{\rm i})\Omega_{\rm p}, \tag{6}$$

where $z' = z/z_0$ , $\alpha_{\rm r} = -\mathrm{Im}[\rho_{41}]\gamma_{41}/\Omega_{\rm p}$, and $\alpha_{\rm i} = \mathrm{Re}[\rho_{41}]\gamma_{41}/\Omega_{\rm p}$. As $\Omega_{\rm s}(x)$ is a function of $x$, $\alpha_{\rm r}$ and $\alpha_{\rm i}$ are also functions of $x$. Equation (6) can be solved analytically to obtain the transmission function of the atomic medium at $z' = L$,

$$T(x) = \mathrm{e}^{\alpha_{\rm r}(x)L}\,\mathrm{e}^{\mathrm{i}\alpha_{\rm i}(x)L}. \tag{7}$$

By Fourier transform of $T(x)$, the Fraunhofer or far-field diffraction equation can be obtained as[17]

$$I_{\rm p}(\theta) = \left|E_{\rm p}^{1}(\theta)\right|^{2}\frac{\sin^{2}(M\pi\Lambda\sin\theta/\lambda_{\rm p})}{M^{2}\sin^{2}(\pi\Lambda\sin\theta/\lambda_{\rm p})}, \tag{8}$$

where

$$E_{\rm p}^{1}(\theta) = \int_{0}^{1} T(x)\exp(-\mathrm{i}2\pi\Lambda x\sin\theta/\lambda_{\rm p})\,\mathrm{d}x \tag{9}$$

corresponds to the Fraunhofer diffraction of a single space period, $M$ is the number of spatial periods of the grating illuminated by the probe beam, and $\theta$ is the diffraction angle of the probe field with respect to the $z$ direction. Here, $\Lambda$ is chosen as the unit for $x$. Since we are mainly interested in the first-order diffraction intensity, we calculate $I_{\rm p}(\theta)$ along the first-order diffraction angle determined by the grating equation, $\sin\theta_1 = \lambda_{\rm p}/\Lambda$, with the result

$$I_{\rm p}(\theta_1) = \left|E_{\rm p}^{1}(\theta_1)\right|^{2}, \tag{10}$$

where

$$E_{\rm p}^{1}(\theta_1) = \int_{0}^{1} T(x)\exp(-\mathrm{i}2\pi x)\,\mathrm{d}x. \tag{11}$$

## 3. Results and discussion

Figure 2 displays the diffraction pattern as a function of $\sin\theta$ for $M = 5$ and $\Lambda/\lambda_p = 4$. The solid and dashed curves represent the diffraction intensity with and without phase modulation, respectively. This clearly shows that the amplitude modulation (dashed curve) gathers more than 90% of the energy into the zeroth-order direction, while little energy is dispersed in high-order directions. When the phase modulation is added (solid curve), more energy is shifted into the first- and second-order directions. With parameters properly chosen as: $\Delta_p = 1.7\gamma_{41}$, $\Delta_c = \Delta_s = 0$, $\Omega_p = 0.1\gamma_{41}$, $\Omega_c = 9.7\gamma_{41}$, $\Omega_s = 0.16\gamma_{41}$, $L = 900$, $\Gamma_{41} = \Gamma_{42} = \Gamma_{43} = 0.66\gamma_{41}$, $\gamma_{42} = \gamma_{43} = \gamma_{41}$, and $\gamma_{31} = \gamma_{32} = \gamma_{21} = 0.004\gamma_{41}$, the first-order diffraction efficiency can be even more than 32%. This is very close to the efficiency of an ideal sinusoidal phase grating, which is approximately 34%.[29] At the same time, the zeroth-order diffraction intensity decreases to about 10%, and about 9% of the energy is dispersed into the second-order direction. In numerical modeling, we find that the first-order diffraction efficiency depends mainly on the Rabi frequencies ($\Omega_c$ and $\Omega_s$), the probe detuning $\Delta_p$, and the interaction length $L$.

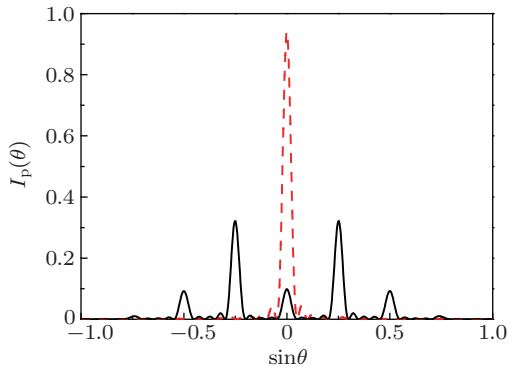



**Fig. 2.** (color online) The diffraction pattern as a function of $\sin\theta$ with (solid curve) and without (dashed curve) phase modulation. The parameters are $\Delta_p = 1.7\gamma_{41}$, $\Delta_c = \Delta_s = 0$, $\Omega_p = 0.1\gamma_{41}$, $\Omega_c = 9.7\gamma_{41}$, $\Omega_s = 0.16\gamma_{41}$, $M = 5$, $L = 900$, $\Lambda/\lambda_p = 4$, $\Gamma_{41} = \Gamma_{42} = \Gamma_{43} = 0.66\gamma_{41}$, $\gamma_{42} = \gamma_{43} = \gamma_{41}$, and $\gamma_{31} = \gamma_{32} = \gamma_{21} = 0.004\gamma_{41}$.

Figure 3 illustrates the first-order diffraction intensity $I_p(\theta_1)$ as a function of $\Omega_s$ with different $\Omega_c$. In curve $a$, the peak value of $I_p(\theta_1)$ is only 7% at $\Omega_s = 0.08\gamma_{41}$ for $\Omega_c = \gamma_{41}$, but it increases dramatically as $\Omega_c$ increases (see curves $b$ and $c$). When $\Omega_c$ increases to $9.7\gamma_{41}$ (curve $c$), the peak value reaches a maximum larger than 32% at $\Omega_s = 0.16\gamma_{41}$. Then it decreases as $\Omega_c$ continues to increase, as shown in curve $d$. In curve $c$, as $\Omega_s$ changes from 0 to $0.16\gamma_{41}$, the first-order diffraction efficiency changes from zero to the maximum value. Therefore, by choosing a proper $\Omega_c$, $I_p(\theta_1)$ can be controlled by changing the intensity of $\Omega_s$, which can be set well below the saturation level ($\Omega_s < \gamma_{41}$). In a word, a weak standing-wave signal field can be used to modulate a weak probe field.

Figure 4 displays the first-order diffraction intensity $I_p(\theta_1)$ as a function of probe detuning $\Delta_p$ with different $L$. The peak value of $I_p(\theta_1)$ only reaches 9% at $\Delta_p = 1.2\gamma_{41}$ when $L$ is 300 (curve $a$), and it increases as $L$ increases (curves $b$ and $c$). The maximum diffraction efficiency (32%) occurs at $\Delta_p = 1.7\gamma_{41}$ when $L$ is 900, as curve $c$ shows. As $L$ continues to increase, the peak value begins to decrease slowly (see curve $d$). Thus, a proper $L$ is necessary to achieve a high diffraction intensity.

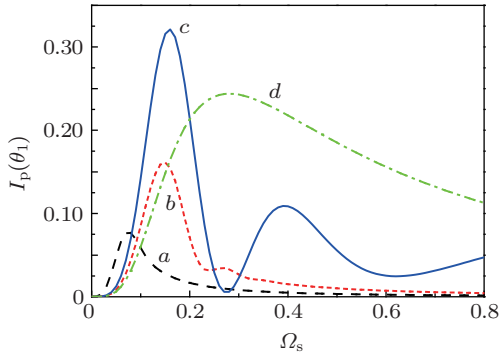



**Fig. 3.** (color online) First-order diffraction intensity $I_p(\theta_1)$ as a function of $\Omega_s$ with different $\Omega_c$. The curves $a$, $b$, $c$, and $d$ represent the cases of $\Omega_c = \gamma_{41}$, $3\gamma_{41}$, $9.7\gamma_{41}$, and $20\gamma_{41}$, respectively. Here, $\Delta_p = 1.7\gamma_{41}$, $\Delta_c = \Delta_s = 0$, $\Omega_p = 0.1\gamma_{41}$, and $L = 900$. Other parameters are the same as those in Fig. 2.

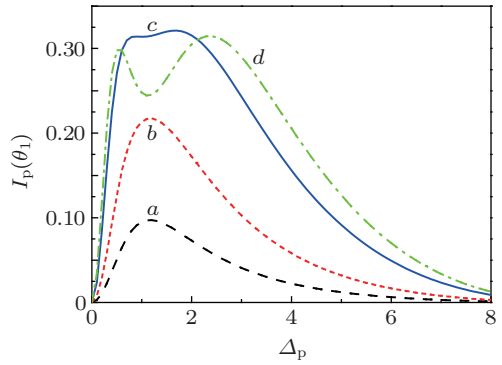



**Fig. 4.** (color online) First-order diffraction intensity $I_p(\theta_1)$ as a function of $\Delta_p$ with different $L$. The curves $a$, $b$, $c$, and $d$ represent the cases of $L = 300$, 500, 900, and 1100, respectively. Here, $\Delta_c = \Delta_s = 0$, $\Omega_p = 0.1\gamma_{41}$, $\Omega_c = 9.7\gamma_{41}$, and $\Omega_s = 0.16\gamma_{41}$. Other parameters are the same as those in Fig. 2.

The values of $\Delta_c$ and $\Delta_s$ have been sought, and we find that the best result occurs at $\Delta_c = \Delta_s = 0$. As a result, when we choose the parameters as: $\Delta_p = 1.7\gamma_{41}$, $\Delta_c = \Delta_s = 0$, $\Omega_p = 0.1\gamma_{41}$, $\Omega_c = 9.7\gamma_{41}$, $\Omega_s = 0.16\gamma_{41}$, and $L = 900$, the best first-order diffraction efficiency is achieved, which is more than 32%. This atomic grating can be realized in a sodium or rubidium medium.

## 4. Conclusion

We have investigated an electromagnetically induced phase grating in a homogeneously broadened medium consisting of a four-level tripod-type atomic system. The re-

sults show that the diffraction efficiency of the phase grating can be controlled easily by changing the intensity of the weak standing-wave signal field. Choosing proper parameters, the first-order diffraction efficiency can reach more than 32% which is very close to that of an ideal sinusoidal phase grating (about 34%). Such a system can be realized in a sodium or rubidium medium, and it could find application in an all-optical switch where a weak standing-wave signal field is used to modulate and switch a weak probe field.

## References


[1] Alzetta G, Gozzini A, Moi L and Orriols G 1976 *Nuovo Cimento B* **36** 5

[2] Alzetta G and Moi L 1979 *Nuovo Cimento B* **52** 209

[3] Gray H R, Whitley R M and Stroud C R 1978 *Opt. Lett.* **3** 218

[4] Boller K J, Imamoglu A and Harris S E 1991 *Phys. Rev. Lett.* **66** 2593

[5] Harris S E 1989 *Phys. Rev. Lett.* **62** 1033

[6] Ling H Y 1994 *Phys. Rev. A* **49** 2827

[7] Scully M O 1991 *Phys. Rev. Lett.* **67** 1855

[8] Scully M O and Zhu S Y 1992 *Opt. Commun.* **87** 134

[9] Kasapi A, Jain M, Yin G Y and Harris S E 1995 *Phys. Rev. Lett.* **74** 2447

[10] Hau L V, Harris S E, Dutton Z and Behroozi C H 1999 *Nature* **397** 594

[11] Bajcsy M, Zibrov A S and Lukin M D 2003 *Nature* **426** 638

[12] Heinze G, Hubrich C and Halfmann T 2013 *Phys. Rev. Lett.* **111** 033601

[13] Deng L, Kozuma M, Hagley E W and Payne M G 2002 *Phys. Rev. Lett.* **88** 143902

[14] Wu Y, Saldana J and Zhu Y 2003 *Phys. Rev. A* **67** 013811

[15] Marte P, Zoller P and Hall J L 1991 *Phys. Rev. A* **44** 4118

[16] Goldner L S, Gerz C, Spreeuw R J C, Rolston S L, Westbrook C I and Phillips W D 1994 *Phys. Rev. Lett.* **72** 997

[17] Ling H Y, Li Y Q and Xiao M 1998 *Phys. Rev. A* **57** 1338

[18] Brown A W and Xiao M 2005 *Opt. Lett.* **30** 699

[19] Dutta B K and Mahapatra P K 2006 *J. Phys. B: At. Mol. Opt. Phys.* **39** 1145

[20] Xiao Z H, Shin S G and Kim K 2010 *J. Phys. B: At. Mol. Opt. Phys.* **43** 161004

[21] de Araujo L E E 2010 *Opt. Lett.* **35** 977

[22] Dong Y B, Wang H H, Gao J R and Zhang J X 2006 *Phys. Rev. A* **74** 063810

[23] Zhao Y T, Zhao J M, Xiao L T, Yin W B and Jia S T 2004 *Chin. Phys. Lett.* **21** 76

[24] Dong Y B, Zhang J X, Wang H H and Gao J R 2006 *J. Phys. B: At. Mol. Opt. Phys.* **39** 3447

[25] Wang L and Hu X M 2004 *Acta Phys. Sin.* **53** 2544 (in Chinese)

[26] Dong Y B, Zhang J X, Wang H H and Gao J R 2006 *Chin. Phys.* **15** 1262

[27] Dong Y B, Dong Y E and Gao J R 2008 *Chin. Phys. B* **17** 3306

[28] Wan R G, Kou J, Jiang L, Jiang Y and Gao J Y 2011 *Phys. Rev. A* **83** 033824

[29] Goodman J W 1968 *Introduction to Fourier Optics* (New York: McGraw-Hill)